Effect of Hole Transport Layer Acceptor Density on the Performance of $FASnI_3$ Perovskite Solar Cells

Muchammad Rizal Pahlevi[1,2], Rossyaila Matsna Muslimawati[3], Mohammad Kemal Agusta[4], Muhammad Haris Mahyuddin[4,*]

[1]Master Program of Engineering Physics, Faculty of Industrial Technology, Institut Teknologi Bandung, Jl. Ganesha 10 Bandung 40132, Indonesia.
[2]Construction Division of Sumatera, Kalimantan, and Sulawesi PT PLN (Persero) Head Office, Jl. Trunojoyo Blok M – I No 135 Jakarta 12160, Indonesia.
[3]Doctoral Program of Engineering Physics, Faculty of Industrial Technology, Institut Teknologi Bandung, Jl. Ganesha 10 Bandung 40132, Indonesia.
[4]Quantum and Nano Technology Research Group, Faculty of Industrial Technology, Institut Teknologi Bandung, Jl. Ganesha 10 Bandung 40132, Indonesia.

*Email: mahyuddin133@itb.ac.id

Abstract. Lead-free perovskites have emerged as a highly promising alternative for efficient and environmentally friendly photovoltaics due to their inherent optoelectronic properties. This study presents a numerical investigation into structured n–i–p inorganic perovskite photovoltaics using the Solar Cell Capacitance Simulator (SCAPS-1D). Various carbon materials, including single-walled carbon nanotubes (SWCNT), graphene oxide (GO), and reduced graphene oxide (rGO), were employed as candidates for the hole transport layer (HTL) with $FASnI_3$ serving as the active material and TiO_2 as the electron transport layer (ETL). This study investigates the impact of acceptor density on the performance of perovskite solar cells (PSCs) using various hole transport layers (HTLs), specifically SWCNT, GO, and rGO. The results indicate that increasing the acceptor density enhances the power conversion efficiency (PCE), with GO showing a PCE increase from 17.99% to 19.61% as the acceptor density rises from $NA=10^{15}$ cm^{-3} to $NA=10^{22}$ cm^{-3}. Additionally, the open circuit voltage (Voc) improves from 0.77 V to 0.83 V, along with an increase in the fill factor (FF) from 85.50% to 86.31%, indicating better charge transport capabilities. In contrast, rGO emerges as the most effective HTL, demonstrating a significant increase in PCE from 29.77% to 30.41%, alongside stable Voc growth from 1.22 V to 1.24 V. The superior charge transport characteristics of rGO, reflected in a higher fill factor that rises from 89.38% to 89.86%, highlight its effectiveness compared to GO. This study emphasizes the critical role of acceptor density in optimizing PSC performance and its significance for future research and the development of advanced HTL materials.

Keywords: *perovskite solar cells; SCAPS-1D simulation; hole transport materials.*

Received _____, Revised _____, Accepted for publication _____

1 Introduction

Solar energy is vital for meeting future global energy demands. Over recent years, single-junction silicon solar cells have dominated the global photovoltaic (PV) market. Currently, crystalline silicon (C-Si) solar cells have achieved a power conversion efficiency (PCE) of 27.6% [1], approaching their theoretical maximum of 33% [2]. However, challenges such as high manufacturing costs and significant space requirements for installation have driven researchers to explore alternatives. One promising development is the emergence of perovskite solar cells (PSCs), which have rapidly advanced, achieving PCEs as high as 25.2% [3]. These efficiencies make PSCs competitive with conventional silicon-based solar cells. The exceptional photovoltaic performance of PSCs is attributed to the unique properties of perovskite materials, combined with continuous optimization in material properties, device architecture, and processing techniques [4]. A key factor in achieving high-performance PSCs is selecting suitable perovskite materials and charge transport layers. Perovskites, widely used as light-absorbing materials, have faced concerns over lead toxicity. Consequently, research has focused on lead-free alternatives, such as those based on Sn^{2+}, Bi^{3+}, Sb^{3+}, and Ge^{2+}. Among these, Sn^{2+}-based perovskites have shown significant promise, with $FASnI_3$ achieving a PCE of 14.81% [5]. The hole transport layer (HTL) is critical in enhancing PSC performance. It facilitates hole extraction and transport, prevents electron backflow to the anode, isolates the perovskite layer from the anode to improve stability, and aids in enhancing the open-circuit voltage (V_{OC}) through proper alignment of the highest occupied molecular orbital (HOMO) energy levels [6].

Acceptor density measures the concentration of acceptor atoms in a semiconductor, typically atoms with one fewer electron than the host material, such as boron in silicon [7]. These acceptors create holes in the energy band structure, enhancing electrical conductivity by increasing the number of charge carriers. However, excessively high acceptor density can disrupt the energy band structure, potentially reducing the mobility of electrons and holes and diminishing conductivity [8].

In this study, SCAPS-1D simulation is utilized to analyze the impact of acceptor density in GO, rGO, and SWCNT as HTLs on the performance of $FASnI_3$-based PSCs with the architecture $FTO/TiO_2/FASnI_3/HTL/C$. The aim is to identify optimal HTL characteristics for achieving high PCEs in lead-free PSCs. The results reveal that acceptor density significantly affects the PCE of $FTO/TiO_2/FASnI_3/GO/C$ but has a smaller impact on systems using SWCNT or rGO as HTLs. This suggests that the composition and structure of the HTL material strongly influence charge carrier transport and recombination processes. For GO-based HTLs, higher acceptor densities likely enhance charge separation

and transport, leading to improved efficiency [9]. Conversely, the SWCNT and rGO system's inherent electronic properties may already be optimized, making further increases in acceptor density less impactful.

2 Methodology

SCAPS-1D version 3.3.10 was employed to simulate and model perovskite solar cells (PSCs) using $FASnI_3$ as the active layer [10]. This software is based on three fundamental semiconductor equations: (1) Poisson's equation, which relates the charge carrier concentration to the electrostatic potential, (2) the continuity equation for electrons, describing the balance between charge carrier generation, drift, and recombination, and (3) continuity equation for holes, similarly outlining the behavior of hole carriers in the semiconductor [11].

The perovskite solar cell configuration simulated in this study is illustrated in Figure 1, consisting of FTO/TiO_2/$FASnI_3$/HTL/Carbon, where the HTL is varied among SWCNT, GO, and rGO. The physical parameters for each material layer (FTO, ETL, active layer, and electrodes) are detailed in Table 1, while the parameters specific to the HTL materials are provided in Table 2. These parameters are derived from multiple references [11], [12], [13], [14]. For the simulation, the thickness of the HTL layer (SWCNT, GO, and rGO) was varied from 0 to 2000 nm, while the shallow acceptor density in the HTL material was adjusted across a range from 1×10^{15} – 1×10^{22} NA (cm^{-3}).

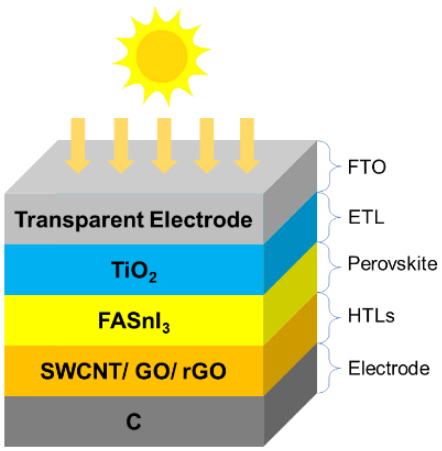

Figure 1 Device structure of Perovskite Solar Cells.

Table 1 Simulation parameter for different layers of PSC

Parameter	FTO	$FaSnI_3$	TiO_2
Thickness, (nm)	500	1000	30
Bandgap, Eg (eV)	3.5	1.41	3.2
Electron affinity, χ (eV)	4.0	4,4	2.05
Dielectric permittivty, εr	9	8.2	3.0
CB effective density of states, Nc (cm^{-3})	2.2×10^{18}	1×10^{18}	2.2×10^{18}
VB effective density of states, Nv (cm^{-3})	1.8×10^{19}	1×10^{18}	1.8×10^{19}
Electron mobility, μn (cm^2/Vs)	20	22	20
Hole mobility, μp (cm^2/Vs)	10	22	10
Shallow donor density, $ND(cm^{-3})$	2×10^{19}	0	1×10^{16}
Shallow acceptor density, $NA(cm^{-3})$	0	1.25×10^{19}	0
Defect density, Nt (cm^{-3})	1×10^{15}	4.6×10^{16}	1×10^{15}
Electron thermal velocity (cm/s)	1×10^{7}	1×10^{7}	1×10^{7}
Hole thermal velocity (cm/s)	1×10^{7}	1×10^{7}	1×10^{7}

Table 2 Simulation parameter of HTLs

Parameter	SCWNT	GO	rGO
Thickness, (nm)	0 – 2000	0 – 2000	0 – 2000
Bandgap, Eg (eV)	1.3	2,48	1,69
Electron affinity, χ (eV)	3.8	2,3	3,56
Dielectric permittivty, εr	10	10	13,3
CB effective density of states, Nc (cm^{-3})	2.9×10^{20}	2.2×10^{18}	1×10^{18}
VB effective density of states, Nv (cm^{-3})	2.9×10^{20}	1.8×10^{19}	1.8×10^{19}
Electron mobility, μn (cm^2/Vs)	1.5	26	26
Hole mobility, μp (cm^2/Vs)	1.5	123	123
Shallow donor density, $ND(cm^{-3})$	0	0	0
Shallow acceptor density, $NA(cm^{-3})$	$10^{15} – 10^{22}$	$10^{15} – 10^{22}$	$10^{15} – 10^{22}$
Defect density, Nt (cm^{-3})	1×10^{15}	1×10^{10}	1×10^{10}
Electron thermal velocity (cm/s)	1×10^{7}	1×10^{7}	1×10^{7}
Hole thermal velocity (cm/s)	1×10^{7}	1×10^{7}	1×10^{7}

All physical parameters used for the structural simulation of PSCs with SCAPS-1D are summarized in Tables 1 and 2. The simulations were conducted at a constant temperature of 300 K, a frequency of 1.0×10^6 Hz, under standard AM 1.5G illumination at 1000 $W.m^{-2}$. Variations in illumination intensity and probe temperature were introduced to evaluate their effects on key photovoltaic parameters such as open circuit voltage (V_{OC}), power conversion efficiency (PCE), short circuit current density (J_{SC}), and fill factor (FF). Additionally, the impact of varying the shallow acceptor density of the hole transport layer (HTL) on these parameters was analyzed. In the SCAPS-1D action panel, the thermal velocity of electrons and holes was set at $1,0 \times 10^7$ cm s^{-1}, and neutral defect

states were assumed. Band-to-band recombination data was excluded from the simulation. A single energy distribution with a characteristic energy of 0.1 eV was used for all layers, and both series resistance (R_S) and shunt resistance (R_{Sh}) were neglected during the initial calculations. Optical reflection at each layer and interface was not considered. The energy level diagram of the PSC layers is illustrated in Figure 2, based on several references [15].

HOMO (Highest Occupied Molecular Orbital) and LUMO (Lowest Unoccupied Molecular Orbital) are fundamental concepts in chemistry and materials science. These levels are critical in understanding electronic properties, particularly in applications such as perovskite solar cells. HOMO represents the highest energy level occupied by electrons, while LUMO is the lowest energy level available for electrons to occupy. The energy difference between these levels, known as the band gap (E_g), determines a material's ability to absorb light and generate electric current. The relationship is expressed as:

$$E_g = E_{LUMO} - E_{HOMO} \quad (1)$$

For perovskite materials like $FASnI_3$, the smaller band gap compared to silicon-based solar cells enhances light absorption across the visible and near-infrared spectrum [16]. Research highlights the importance of designing materials with optimized HOMO and LUMO levels to improve PSC efficiency [17]. The PSC configuration modeled in this study includes FTO/TiO_2/$FASnI_3$/(SWCNT, GO, or rGO as HTL)/Carbon. The physical parameters for each material layer, including the FTO, ETL, active layer, and electrodes, are detailed in Table 1. Specific HTL parameters are shown in Table 2, derived from multiple references. A plane-wave basis set with a cutoff energy of 500 eV was used for calculations. Brillouin zone sampling centered at the Γ-point was set to 1×1×1 following the Monkhorst-Pack scheme [18]. To account for dispersion corrections, the zero-damping D3 method was applied. Cell optimizations were conducted using the conjugate gradient method, and convergence was achieved when the maximum forces on each atom were below 0.01 eV/A˚. During these calculations, all atoms were allowed to fully relax.

3 Results and Discussion

3.1 Acceptor Density Effect

The test results presented in Figure 2 demonstrate the effect of varying acceptor density (N_A) on the performance of perovskite solar cells (PSCs) utilizing different hole transport layer (HTL) materials. For SWCNT, the change in acceptor density led to moderate performance improvement. The power conversion efficiency (PCE) increased from 26.45% at N_A = 1×10^{15} cm^{-3} to

27.15% at N_A = 1×22^{15} cm^{-3}. However, the open-circuit voltage (V_{OC}) exhibited slight fluctuations, decreasing from 1.16 V to 1.15 V, suggesting that although efficiency improved, the voltage stability for SWCNT was suboptimal compared to other materials. The short-circuit current density (J_{SC}) remained steady at 27.16 mA/cm^2, indicating minimal impact from changes in acceptor density. Notably, the fill factor (FF) increased significantly from 83.80% to 86.59%, reflecting enhanced charge transport with higher N_A.

For GO, an increase in acceptor density also positively influenced device efficiency, though the impact was less pronounced compared to rGO. The PCE improved from 17.99% at N_A = 1×10^{15} cm^{-3} to 19.61% at N_A = 1×10^{22} cm^{-3}. The V_{OC} increased from 0.77 V to 0.83 V, indicating enhanced voltage generation capacity with higher N_A. Similar to SWCNT, the J_{SC} remained constant at 27.30 mA/cm^2, demonstrating stable current generation. The FF improved slightly, from 85.50% to 86.31%, indicating better charge transport. Despite these improvements, GO exhibited lower overall performance and voltage stability than rGO. Among the materials studied, rGO as an HTL demonstrated the best performance. The PCE showed a significant increase from 29.77% at N_A = 1×10^{15} cm^{-3} to 30.41% N_A = 1×10^{22} cm^{-3}, marking the highest efficiency among the three materials. The V_{OC} also exhibited stable growth, increasing from 1.22 V to 1.24 V, highlighting strong voltage stability with increased acceptor density. The J_{SC} remained unchanged at 27.31 mA/cm^2, consistent with other materials. However, rGO outperformed in terms of FF, with an increase from 89.38% to 89.86%, underscoring its superior charge transport capability.

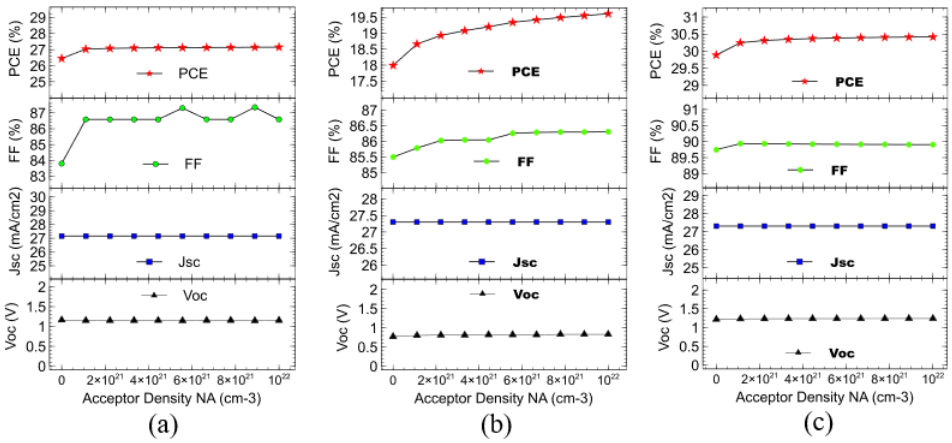

Figure 2 The impact of the HTLs acceptor density for different materials (a) SWCNT, (b) GO, and (c) rGO

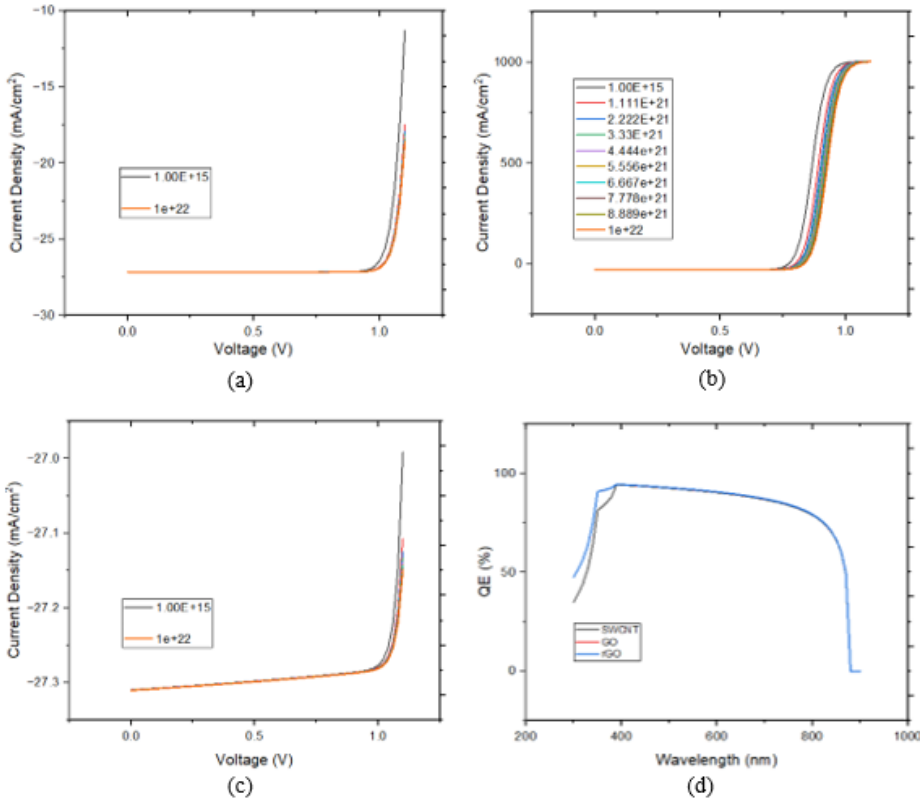

Figure 3 The J–V characteristic curve for different materials (a) J-V SWCNT, (b) J-V GO, (c) J-V rGO, and (d) QE

The J-V curve presented in Figure 3 illustrates the effect of varying acceptor density on current transport performance in SWCNT, GO, and rGO. For SWCNT, an increase in acceptor density from $1\times10^{15}\,cm^{-3}$ to $1\times10^{22}\,cm^{-3}$ results in a higher current under forward bias, exhibiting an exponential rise as the voltage approaches 1 V. A similar trend is observed in GO and rGO, where higher acceptor densities also lead to increased current, albeit with slight performance variations among the materials. In terms of Quantum Efficiency (QE), rGO achieves the highest photon-to-current conversion efficiency across various wavelengths, nearing 100% in certain spectral ranges. Conversely, GO and SWCNT exhibit lower efficiencies, particularly at longer wavelengths, while maintaining strong performance at shorter wavelengths (approximately 400 nm). Overall, rGO demonstrates superior photon-to-electron conversion efficiency and a more consistent response to changes in acceptor density compared to SWCNT and GO.

The primary factor contributing to rGO's superior efficiency and performance among the three HTL materials, concerning acceptor density, is its exceptional charge transport and voltage stability. Its structural properties enable high electrical conductivity, optimizing charge collection and flow, which significantly enhances its power conversion efficiency (PCE). Furthermore, rGO consistently improves both the open-circuit voltage (V_{OC}) and fill factor (FF), effectively reducing energy losses and further solidifying its status as the most efficient material in this study.

3.2 Band Alignment Analysis

The band alignment diagram for various HTLs is shown in Figure 4, highlighting their interaction with the perovskite active layer, $FASnI_3$. The highest occupied molecular orbital (HOMO) level of $FASnI_3$ is located at approximately -5.61 eV, which is notably lower than the HOMO levels of the HTLs under consideration: SWCNT at -5.1 eV, GO at -4.9 eV, and rGO at -5.3 eV. This energy difference creates a significant driving force for hole extraction from the perovskite layer, thereby enabling efficient hole transfer to the respective HTL materials.

For SWCNT, the HOMO level of -5.1 eV supports effective hole transport, although its driving force for hole extraction is slightly weaker compared to rGO, whose HOMO level of -5.3 eV is better aligned with that of $FASnI_3$. This closer alignment enhances the efficiency of hole transfer from the perovskite layer. Conversely, GO, with its HOMO at -4.9 eV, exhibits a less favorable energy alignment. This mismatch could hinder hole extraction efficiency, negatively impacting the solar cell's overall performance.

Regarding the lowest unoccupied molecular orbital (LUMO) levels, the values are as follows: SWCNT at -3.8 eV, rGO at -3.6 eV, and GO at -2.3 eV. Both SWCNT and rGO have LUMO levels that align well with the electron energy levels in the perovskite layer, allowing smooth electron transport with minimal energy loss during the hole transport process. However, the significantly higher LUMO level of GO at -2.3 eV increases the likelihood of electron recombination, which can reduce GO’s effectiveness as an HTL and diminish the solar cell's efficiency. Proper energy level alignment between the perovskite layer and HTLs is critical for optimizing charge carrier dynamics, minimizing recombination, and enhancing the overall performance of perovskite solar cells (PSCs).

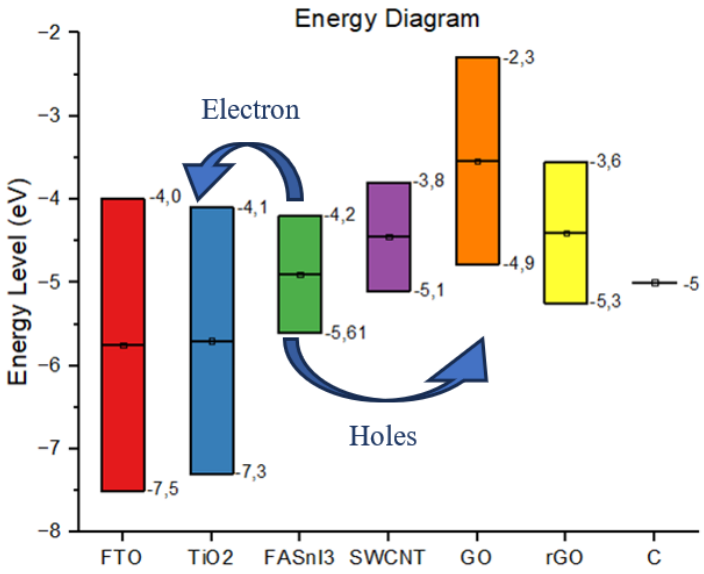

Figure 4 Energy levels materials FTO, TiO_2, $FASnI_3$, HTL variation (SWCNT, GO, rGO), and Carbon on the parameters in Table 1 and Table 2 [11], [12], [13], [14].

4 Conclusion

Acceptor density is a key factor influencing the performance of perovskite solar cells (PSCs) with various materials used as hole transport layers (HTLs). The analysis results show that increasing the acceptor density significantly enhances the power conversion efficiency (PCE) in all studied materials, including SWCNT, GO, and rGO. In the case of SWCNT, while the PCE increases, fluctuations in the open circuit voltage (Voc) indicate that stability can be challenging. GO also shows an increase in efficiency, but it remains lower compared to rGO, demonstrating stable growth in Voc and better overall performance. rGO is found to be the superior material regarding acceptor density, showing the highest PCE, good voltage stability, and superior charge transport capability. The increase in acceptor density not only enhances efficiency but also contributes to reducing energy losses in the system. Thus, acceptor density plays an important role in optimizing PSC performance and serves as a focal area for further research and the development of more effective HTL materials.

5 References

[1] N. Renewable Energy Laboratory, “NREL Best Research-Cell Efficiency Chart,” 2024.

[2] A. R. Zanatta, "The Shockley–Queisser limit and the conversion efficiency of silicon-based solar cells," *Results in Optics*, vol. 9, Dec. 2022, doi: 10.1016/j.rio.2022.100320.

[3] L. C. Andreani, A. Bozzola, P. Kowalczewski, M. Liscidini, and L. Redorici, "Silicon solar cells: Toward the efficiency limits," Jan. 01, 2019, *Taylor and Francis Ltd.* doi: 10.1080/23746149.2018.1548305.

[4] M. A. Green, A. Ho-Baillie, and H. J. Snaith, "The emergence of perovskite solar cells," 2014, *Nature Publishing Group*. doi: 10.1038/nphoton.2014.134.

[5] B. Bin Yu *et al.*, "Heterogeneous 2D/3D Tin-Halides Perovskite Solar Cells with Certified Conversion Efficiency Breaking 14%," *Advanced Materials*, vol. 33, no. 36, Sep. 2021, doi: 10.1002/adma.202102055.

[6] J. Santos *et al.*, "Hole-Transporting Materials for Perovskite Solar Cells Employing an Anthradithiophene Core," *ACS Appl Mater Interfaces*, vol. 13, no. 24, pp. 28214–28221, Jun. 2021, doi: 10.1021/acsami.1c05890.

[7] W. Setyawan and S. Curtarolo, "High-throughput electronic band structure calculations: Challenges and tools," *Comput Mater Sci*, vol. 49, no. 2, pp. 299–312, Aug. 2010, doi: 10.1016/j.commatsci.2010.05.010.

[8] Y. Zhang and J. Wang, "Bound exciton model for an acceptor in a semiconductor," *Phys Rev B Condens Matter Mater Phys*, vol. 90, no. 15, Oct. 2014, doi: 10.1103/PhysRevB.90.155201.

[9] G. Ortiz *et al.*, "Impact of acceptor concentration on electrical properties and density of interface states of 4H-SiC n-metal-oxide-semiconductor field effect transistors studied by Hall effect," *Appl Phys Lett*, vol. 106, no. 6, 2015, doi: 10.1063/1.4908123ï.

[10] M. K. Hossain, M. H. K. Rubel, G. F. I. Toki, I. Alam, M. F. Rahman, and H. Bencherif, "Effect of Various Electron and Hole Transport Layers on the Performance of CsPbI3-Based Perovskite Solar Cells: A Numerical Investigation in DFT, SCAPS-1D, and wxAMPS Frameworks," *ACS Omega*, vol. 7, no. 47, pp. 43210–43230, Nov. 2022, doi: 10.1021/acsomega.2c05912.

[11] L. R. Karna, R. Upadhyay, and A. Ghosh, "All-inorganic perovskite photovoltaics for power conversion efficiency of 31%," *Sci Rep*, vol. 13, no. 1, Dec. 2023, doi: 10.1038/s41598-023-42447-w.

[12] A. L. Palma *et al.*, "Reduced graphene oxide as efficient and stable hole transporting material in mesoscopic perovskite solar cells," *Nano Energy*, vol. 22, pp. 349–360, Apr. 2016, doi: 10.1016/j.nanoen.2016.02.027.

[13] P. Fooladvand, M. Eskandari, D. Fathi, and N. Das, "Single-walled carbon nanotube as hole transport layer in perovskite solar cell: Efficiency enhancement," *Energy Reports*, vol. 10, pp. 3652–3664, Nov. 2023, doi: 10.1016/j.egyr.2023.10.020.

[14] M. K. A. Mohammed *et al.*, "Improving the performance of perovskite solar cells with carbon nanotubes as a hole transport layer," *Opt Mater (Amst)*, vol. 138, Apr. 2023, doi: 10.1016/j.optmat.2023.113702.
[15] M. K. Hossain *et al.*, "Numerical Analysis in DFT and SCAPS-1D on the Influence of Different Charge Transport Layers of CsPbBr3 Perovskite Solar Cells," *Energy and Fuels*, vol. 37, no. 8, pp. 6078–6098, Apr. 2023, doi: 10.1021/acs.energyfuels.3c00035.
[16] S. D. Stranks *et al.*, "Electron-hole diffusion lengths exceeding 1 micrometer in an organometal trihalide perovskite absorber," 2013. doi: 10.1126/science.1243982.
[17] Q. Chen *et al.*, "Planar heterojunction perovskite solar cells via vapor-assisted solution process," *J Am Chem Soc*, vol. 136, no. 2, pp. 622–625, Jan. 2014, doi: 10.1021/ja411509g.
[18] H. J. Monkhorst and J. D. Pack, "Special points for Brillonin-zone integrations*," 1976.

Acknowledgment

The authors are grateful to PT. PLN (Persero) for the financial and scholarship support provided throughout this research.